Prediction and Optimization of Sulphur Trioxide Yield from Calcination of Aluminium Sulfate Using Central Composite Design

Olumide Olu Olubajo [1], **Isa Yusuf Makarfi** [2]

[1] Abubakar Tafawa Balewa University
Dass road, P. M. B. 0248, Bauchi, 740272, Nigeria

[2] Durban University of Technology
P. O. Box 1334, Durban, 4000, South Africa

DOI: 10.22178/pos.51-2

LCC Subject Category: QD1-65

Received 28.09.2019
Accepted 28.10.2019
Published online 31.10.2019

Corresponding Author:
Olumide Olu Olubajo
ooolubajo@atbu.edu.ng

Abstract. Sulphur trioxides are common toxic gaseous pollutants which can be produced from alternative routes via calcination of aluminum sulfate derived from kaolin clay. Its demand increases geometrically, thus the need to optimize the yield of SO_3 from the calcination of alum is essential. The rate of alum decomposition was monitored by the formation of SO_3 via thermogravimetric analysis and X-ray fluorescence analysis. This study aimed to evaluate the effect of calcination temperature and curing time on the SO_3 conversion and yields using Face Central Composite Design and optimize the process conditions to evaluate the maximum yield of SO_3 using response surface methodology and its effects and interactions were investigated between 800–900 °C at 60-180 minutes. Results indicated that experimental data satisfied second order polynomial regression model for SO_3 conversion and SO_3 yield from TG analysis while XRF analysis satisfied first order model respectively. An increase in SO_3 conversion and yields was observed as the calcination temperature and time were increased both independently and simultaneously. The calcination temperature was found to have a stronger influence compared to the calcination time. Validation indicated agreement between experimental and predicted values with a regression value of 97.8 %, 97.77 % and 97.67 % for SO_3 conversion, SO_3 yield via TG and XRF analyses respectively. Based on the ANOVA, the SO_3 yield via XRF produced the best model with R^2_{pred} of 91.98% while SO_3 yield via TG analysis and SO_3 conversion had R^2_{pred} of 79.99% and 78.01% respectively. Optimization of the production of SO_3 was carried out and the optimal condition for SO_3 conversion, SO_3 yield via TG and XRF analyes were 90.11 %, 91.67 % and 75.81 % respectively at an optimal calcination temperature of 877.43 °C and time of 155.04 minutes respectively.

Keywords: Calcination temperature and time; Conversion; Face central composite design; Sulphur trioxide; Yield.

INTRODUCTION

Sulphur trioxide is invisible odourless but corrosive gas which is considered as an environmental pollutant [1, 2]. It can be produced in an industrial scale as a precursor to sulphuric acid which has numerous industrial applications. Sulphur trioxide is an essential reagent required in sulphonation reactions. Sulfonation and sulfation are major industrial chemical processes used to make a diverse range of products, including dyes and color intensifiers, pigments, medicinal, pesticides and organic intermediates [3]. The most common production route of SO_3 is the catalytic oxidation of sulphur dioxide which is formed from the oxidation of sulphur containing fossil fuels and industrial processes that treats and produces sulfur containing compounds [4]. Several routes for the production of SO_3, among which the decomposition of aluminium sulfate has been considered suitable from [5] research work in which the calcination of aluminum sulfate was achieved by heating at temperature between 700-900 °C and time interval 60–180 minutes. Despite the high efficiency of the production of SO_3 via catalytic oxidation of SO_2., the high cost of catalyst maintainace as well as the corrosive nature of sulphur dioxide are some of its demerits [4]. The thermal decomposition of aluminum sulfate results in the yield of sulphur trioxide which can be influenced by the calcination temperature, time and particle size of the aluminium sulfate in which the particle size was considered to be constant.

Optimization is an essential technique employed in improving the existing condition of a process [6] such as sulphur trioxide (SO_3) production and can be achieved through the use of Response Surface Methodology (RSM). The optimization involves either variation of a given parameter per unit time while the other parameter is held constant using RSM. Its techniques can be employed to establish functional relationships between responses of interest and some inputs [7] and based on their relationships, the dependent variables can be used to predict responses that can be compared with the experimental values [8]. The use of RSM cannot be overemphasized as it assists in the evaluation of several parameters simultaneously with their interactions by limiting the number of an experiment to be conducted, as well as optimize process parameters and estimation of interactions [9, 10]. Central Composite Design (CCD) is amongst one of the several techniques of RSM employed to design experimental procedures which have the advantage of screening a wide range of parameters as well as evaluating single variable/ cumulative effect of the variables to response [11]. It can also determine the number of the experiment to be able to evaluate for optimization of variables and responses [12] and has been found to widely used for the optimization techniques for calcination processes to produce significantly better models compared to other models [13].

An understanding of the interaction of the factors is essential in evaluating their relationship because their interactions are difficult to be determined using the one-factor-at-a-time approach [14]. The three stages in implementing response surface techniques include the design of experiment i.e. Box- Behnken or Central Composite Design (CCD), development of a model equation through statistical and regression analysis and finally optimization of parameters via model equation [15]. RSM has found applications in numerous experimental designs ranging from palm oil transesterification [16], extraction processes [8], drilling process [17], biodiesel production [18], prediction of blended cement properties [19, 20, 21] and decomposition as well as other areas of engineering.

The aim of this paper is to investigate the effect of aluminum sulfate calcination temperature and time on the production of SO_3 through response surface methodology using central composite design (CCD) and interactions studied. The comparison of the SO_3 yields via TG and XRF techniques and SO_3 conversion to ascertain which produces the best yield. It also involves optimization of the process conditions for the production of SO_3 from the decomposition of aluminium sulfate derived from kaolin.

EXPERIMENTAL DESIGN

The summary of the design for responses; Sulphur trioxide conversion and yield estimation for XRF and TG values with calcination temperature and time as factors. The following parameters were chosen as independent variables: calcination temperature (800 ˚C, 850 ˚C, 900 ˚C), while the calcination time (60 min, 120 min, 180 min). Face central composite factorial design (3 level 2 factors) with 9 runs (1 block) (design expert 6.0) where -1 denotes low value of the independent variable (800 ˚C, 60 min), 0 used for the medium value (850 ˚C, 120 min) and the high value (900 ˚C, 180 min) were employed to investigate the effect of the above factors on the responses. A model was fitted to the response surface generated by the experiment.

$$Y_k = f(\textit{Calcination temperature}, \textit{Calcination time}), \quad (1)$$

Design-Expert 6.0.8 software was employed to analyze the best fit data and to estimate the optimal value of the factors considered. RSM was used to determine the optimal process parameters to obtain maximum SO_3 content. CCD at 3 levels, 2 factors was selected as independent variables and the interaction of variables were estimated. 9 runs were carried out to fit the general model of equation (1) and to obtain economically optimum conditions for the SO_3 removal efficiency.

$$Y = \beta_0 + \sum_{i=1}^{k}\beta_i x_i + \sum_{i=1}^{k}\beta_i x_i^2 + \sum_{i=1(i\neq j)}^{k}\beta_{ij} x_i x_j, \quad (2)$$

Where Y is the SO_3 yield, β_o is the coefficient constant, β_i is the linear coefficient, β_{ii} quadratic coefficient effect, β_{ij} is the interaction coefficient effect and $X_i X_j$ is the coded values of variable *i* and *j* respectively. Y_1, Y_2, Y_3 denotes SO_3 conversion, SO_3 yield via TG and XRF analyses respectively. X_1 is the calcination temperature and X_2 is calcination time.

Table 1 indicates the experimental results for the determination of the SO_3 content via Thermogravimetric (TG) analysis and X-ray Fluorescence (XRF) analysis obtained from the calcination of alum derived kaolin to investigate its effect of calcination temperature and time on the SO_3 formation. The statistical analysis of the results was carried out by ANOVA to evaluate the model and its parameters were tabulated in Table 2.

The statistical significance was achieved by the F-test of the experimental result obtained. The model terms were selected or rejected based on the probability value with 95 % confidence level. Then, the response surface contour plots are generated to visualize the individual and the interactive effects of the variables.

Table 1 – Experimental Design and Results

Run	***Temp °C, X_1***	***Time min, X_2***	***Conversion %, Y_1***	***$SO_{3\ TGA}$ %, Y_2***	***$SO_{3\ XRF}$ %, Y_3***
1	800	60	8.30	7.55	6.33
2	800	120	12.60	12.97	8.63
3	800	180	16.97	17.46	11.59
4	850	60	48.55	49.95	25.62
5	850	120	68.29	70.25	45.91
6	850	180	80.16	82.47	57.28
7	900	60	97.40	94.44	93.75
8	900	120	97.40	97.26	95.49
9	900	180	97.40	97.36	97.23

Face central composite design was employed and the factors required include calcination temperature (X_1) and time (X_2) with the responses; SO_3 conversion (Y_1) and SO_3 yield from TG (Y_2) and XRF (Y_3) analyses. The factors and the response variables were investigated and the effect of the various factors on the responses were determined using design expert 6.0.8. Results indicated that a quadratic equation was obtained for SO_3 conversion and SO_3 yield from TG analysis whereas SO_3 yield from XRF analysis satisfied linear model:

$$Y_1 = -4037.45 + 8.67X_1 + 0.86X_2 - 0.0045X_1^2 - 0.000563X_2^2 - 0.0072X_1X_2 \quad (3)$$

$$Y_2 = -4663.90 + 10.172X_1 + 0.79X_2 - 0.0055X_1^2 - 0.00057X_2^2 - 0.0058X_1X_2 \quad (4)$$

$$Y_3 = -701.79 + 0.86X_1 + 0.11X_2 \quad (5)$$

The Equations (3) to (5) represent quantitative effect of the factor variables; calcination temperature and time (X_1, X_2) and their interactions on the response; SO_3 conversion and SO_3 yield from TG and XRF values (Y_1, Y_2, Y_3). The values of X_1 and X_2 were substituted in the equation to obtain the theoretical value of Y_1 Y_2 and Y_3 respectively. Based on the experimental design and factor combination, linear model was found to be significant for SO_3 via XRF analysis amongst other responses which were significant for quadratic models.

Table 2 indicates the analysis of variance (ANOVA) for SO_3 conversion, SO_3 yield from TG analysis and SO_3 yield from XRF analysis, all gave F value for lack of fit was 2.34, 2.33 and 1.53 respectively which also confirms that the models are significant due to the fact that it has an insignificant lack of fit. Table 2 also indicates the model F values for SO_3 conversion, SO_3 yield for TG and SO_3 yield for XRF are 62.54, 69.16 and 125.09 respectively, thus the models are significant implying that there is 0.01% possibility that the noise will be large.

Tables 3-5 indicate that the Predicted R^2 value for the three responses were in logical conformity with the adjusted R^2 value for determination of the 3 responses. The several models produced adequate precision ratios indicating a desirable signal which was greater than 4 [22].

Table 2 – ANOVA for Response Surface Quadratic Model Analysis of Variance for Conversion and Percentage SO_3 Yield for XRF & TG analyses with Central Composite Design CCD

Source	*Sum of Squares*	*DF*	*Mean Square*	*F Value*	*Prob > F*
Model Y_1	11558.43	5	2311.69	62.54	< 0.0001
X_1	10780.62	1	10780.62	291.65	< 0.0001
X_2	270.41	1	270.41	7.32	0.0304
X_1^2	357.8	1	357.8	9.68	0.0171
X_2^2	11.35	1	11.35	0.31	0.5968
X_1X_2	18.79	1	18.79	0.51	0.4989
Residual	258.75	7	36.96		
Lack of Fit	258.75	3	86.25	2.34	0.8240
Model Y_2	11567.17	5	2313.43	69.16	< 0.0001
X_1	10506.86	1	10506.86	314.08	< 0.0001
X_2	342.77	1	342.77	10.25	0.015
X_1^2	512.73	1	512.73	15.33	0.0058
X_2^2	17.68	1	17.68	0.53	0.4908
X_1X_2	12.22	1	12.22	0.37	0.5647
Residual	234.17	7	33.45		
Lack of Fit	234.17	3	78.06	2.33	0.8240
Model Y_3	11531.76	2	5765.88	125.09	< 0.0001
X_1	11259.73	1	11259.73	244.29	< 0.0001
X_2	272.03	1	272.03	5.09	0.0355
Residual	460.93	10	46.09		
Lack of Fit	460.93	6	76.82	1.53	0.1176

Table 3 – Model Summary Statistics/ Sequential Model Sum of Squares for CCD for SO_3 Conversion

Source	*Linear*	*2FI*	*Quadratic*	*Cubic*
Sum of Squares	11051.04	18.79	**4.88.60**	247.98
DF	2	1	**2**	2
Mean square	5525.52	18.79	**244.3**	123.99
F value	72.12	0.23	**6.61**	57.54
Prob> F	< 0.0001	0.6406	**0.0244**	< 0.0004
Std. Dev.	8.75	9.11	**6.08**	1.47
R^2	0.9352	0.9368	**0.9781**	0.9908
Adj. R^2	0.9222	0.9157	**0.9625**	0.9978
Pred. R^2	0.87173	0.752	**0.7801**	0.8941
PRESS	1516.96	2930.38	**2598.21**	1251.95
	Suggested		**Suggested**	Aliased

Authors [23] and [24] reported that a fitted model is said to be acceptable when the R^2 is not less than 80% and greater than 75 % respectively. In this study, the predicted values for developed models had a good correlation with the experimental results as shown in Table 3 indicated R^2 values for 97.81 %, 98.02 % and 96.16 % respectively while R^2_{adj} value for SO_3 conversion, SO_3 yield via TG and XRF analyses were 96.25 %, 96.60 % and 95.39 % respectively, indicating appropriateness of the developed model in predicting the SO_3 conversion, SO_3 yield via TG and XRF analyses for the two factors with R^2 and R^2_{adj} value close to unity. Authors [25] and [26] stated that a better empirical model fit was obtained with the experimental data when the R^2 value is close to unity and observed that a relatively high R^2 value does not imply that the model is adequate, thus, [25] suggested that a R^2_{adj} of above 90% is most appropriate to evaluate the model adequacy for the three responses which were closer to unity. Thus, indicating a good fit of the model to experimental results.

The analysis of variance showed the significant effect of the independent variables on the responses and determine the responses which were significantly affected by the various interactions. The following model terms X_1, X_2, X_1^2 were considered significant while the model terms greater than 0.10 were considered not significant for experimental SO_3 conversion and SO_3 yield via TG analysis whereas, SO_3 yield via XRF analysis showed that only the linear model terms X_1, X_2 were considered significant. The calcination temperature, (X_1) obtained a F value of 291.65, 314.08 and 244.29, while for the calcination time (X_2) produced a F value of 7.32, 10.25 and 5.09 for the experimental SO_3 conversion, SO_3 yield for TG and XRF analyses respectively. The high F values are a strong indication that the effect of the calcination temperature is far more significant compared to the calcination time for all the models. The quadratic term of the temperature obtained a F values of 9.68 and 15.33 respectively with p values falling within $p< 0.05$ or $p < 0.10$ respectively. The quadratic term of the calcination time as well as the product of the calcination temperature and time obtained low F values, thus indicating that their effect is insignificant for the first two responses. It could be concluded that both factors X_1 and X_2 significantly affected the three responses.

Table 4 – Model Summary Statistics/ Sequential Model Sum Of Squares for CCD for SO_3 Yield with TG analysis

Source	***Linear***	***2FI***	***Quadratic***	***Cubic***
Sum of Squares	10849.63	12.22	**705.32**	227.42
DF	2	1	**2**	2
Mean square	5424.82	12.22	**352.66**	113.71
F value	57	0.12	**10.54**	84.28
Prob> F	< 0.0001	0.7401	**0.0077**	0.0001
Std. Dev.	9.76	10.22	**5.78**	1.16
R^2	0.9194	0.9204	**0.9802**	0.9994
Adj. R^2	0.9032	0.8939	**0.966**	0.9986
Pred. R^2	0.8403	0.6755	**0.7999**	0.9336
PRESS	1884.27	3829.56	**2361.51**	783.86
	Suggested		**Suggested**	Aliased

From the experimental results, statistical testing was carried out employing Fishers test for ANOVA and the statistical significance of the second-order model indicated that the regression is statistically significant ($P<0.0001$) for the first two responses while the third response statistical data satisfied linear model; however, the lack of fit is not statistically significant at 99% confidence level, thus the residual variance for the models were insignificant [27, 28]. The analysis of variance indicated significant effect of the independent variables on the responses.

Table 5 – Model Summary Statistics/ Sequential Model Sum of Squares for CCD for SO_3 Yield with XRF values

Source	***Linear***	***2FI***	***Quadratic***	***Cubic***
Sum of Squares	**11531.76**	0.79	197.1	248.28
DF	**2**	1	2	2
Mean square	**5765.88**	0.79	98.55	124.14
F value	**125.09**	0.015	2.62	42.08
Prob> F	**< 0.0001**	0.9037	0.1412	< 0.0007
Std. Dev.	**6.79**	7.15	6.13	1.72
R^2	**0.9616**	0.9616	0.9781	0.9988
Adj. R^2	**0.9539**	0.9488	0.9624	0.997
Pred. R^2	**0.9198**	0.8478	0.7808	0.8571
PRESS	**962.12**	1830.36	2628.47	1714.22
	Suggested			Aliased

Normal Probability and Predicted vs Actual Plots. Figures 1 (b), 2 (b) and 3 (b) also indicated that there is a strong relationship between the predicted and actual values for SO_3 conversion, SO_3 yield for TG and XRF values respectively based on the results obtained.

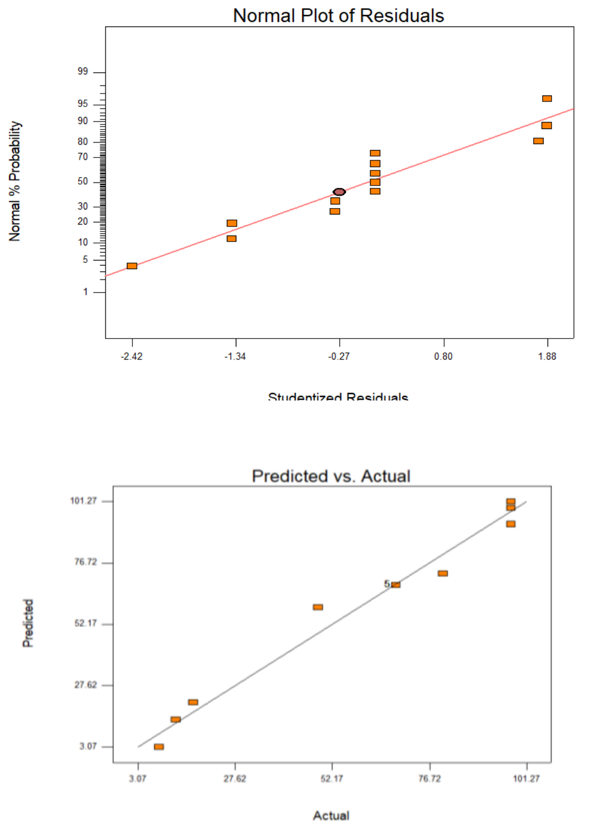

Figure 1 – (a) Normal Plot of residuals indicating significance of the model developed for SO_3 conversion and (b) Predicted vs Actual plot of the model developed for SO_3 conversion

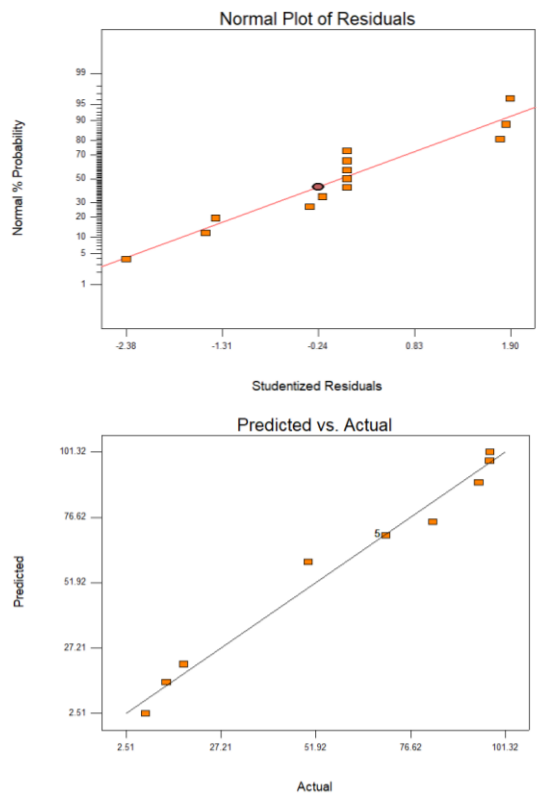

Figure 2 – (a) Normal Plot of residuals indicating significance of the model developed for SO_3 yield with TG analysis and (b) Predicted vs Actual plot of the model developed for SO_3 yield with TG analysis

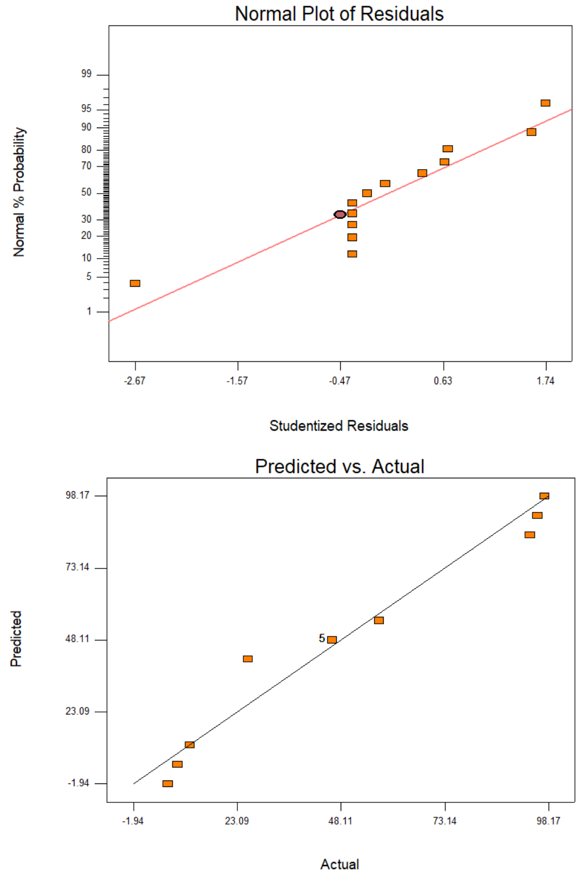

Figure 3 – (a) Normal Plot of residuals indicating significance of the model developed for SO_3 yield with XRF and (b) Predicted vs Actual plot of the model developed for SO_3 yield with XRF

It could be inferred that the predicted model obtained from the Design Expert software was significantly adequate in predicting SO_3 conversion and SO_3 yield for TG and XRF values respectively. Tables 6–8 illustrate the predicted values, actual values and residual errors of SO_3 conversion and SO_3 yield via TG and XRF analyses respectively.

Table 6 – Diagnotistic Case Statistics for SO_3 Conversion

Temp °C	***Time min***	***Actual value %***	***Predicted Value %***	***Resid ual %***
800	60	8.3	3.07	5.23
800	120	12.6	13.97	-1.37
800	180	16.97	20.83	-3.86
850	60	48.55	59	-10.45
850	120	68.29	67.74	0.55
850	180	80.16	72.43	7.73
900	60	97.4	92.18	5.22
900	120	97.4	98.75	-1.35

Table 7 – Diagnotistic Case Statistics for SO_3 Yield via TG Analysis

Temp °C	***Time min***	***Actual value %***	***Predicted Value %***	***Re-sidual %***
800	60	7.55	2.51	5.04
800	120	12.97	14.35	-1.38
800	180	17.46	21.12	-3.66
850	60	49.95	59.73	-9.78
850	120	70.25	69.82	0.43
850	180	82.47	74.85	7.62
900	60	94.44	89.7	4.74
900	120	97.26	98.04	-0.78

Table 8 – Diagnotistic Case Statistics for SO_3 Yield via XRF Analysis

Temp °C	***Time min***	***Actual value %***	***Predicted Value %***	***Re-sidual %***
800	60	6.33	-1.94	8.27
800	120	8.63	4.79	3.84
800	180	11.59	11.53	0.064
850	60	25.62	41.38	-15.76
850	120	45.91	48.11	-2.2
850	180	57.28	54.85	2.43
900	60	93.75	84.7	9.05
900	120	95.49	91.43	4.06

Contour and 3D Plots. The correlation between the responses and the factors were further explained via contour and response surface plots. The diagnostic plots represented by Figures 4–6 employed to estimate the adequacy of the regression model which shows the response plots (3D) and the contour plots for the effect of factors X_1 (calcination temperature), X_2 (calcination time) on the first response Y_1 (SO_3 conversion), second response Y_2 (SO_3 yield with TG analysis) and third response Y_3 (SO_3 yield with XRF analysis) respectively. The response surface curves illustrate the interaction between the factors and determination of the optimal level of the factors for maximum response. The non-parabolic nature of contours implies no significant interaction between both factors [29] as observed in Figure 6.

The calcination temperature and time both caused an increase in the SO_3 conversion and yield % when their values were increased from lower level to higher level as observed from the 3D surface plots. The plotted response surface curves were employed to elucidated the interaction of the factors and to determine the optimal level of each factor for a maximum response. From the predictive model, an increase in the calcination temperature from 800–900 °C at constant time of 60, 120 and 180 minutes led to a significant increase in the SO_3 conversion respectively as illustrated in Figure 7.

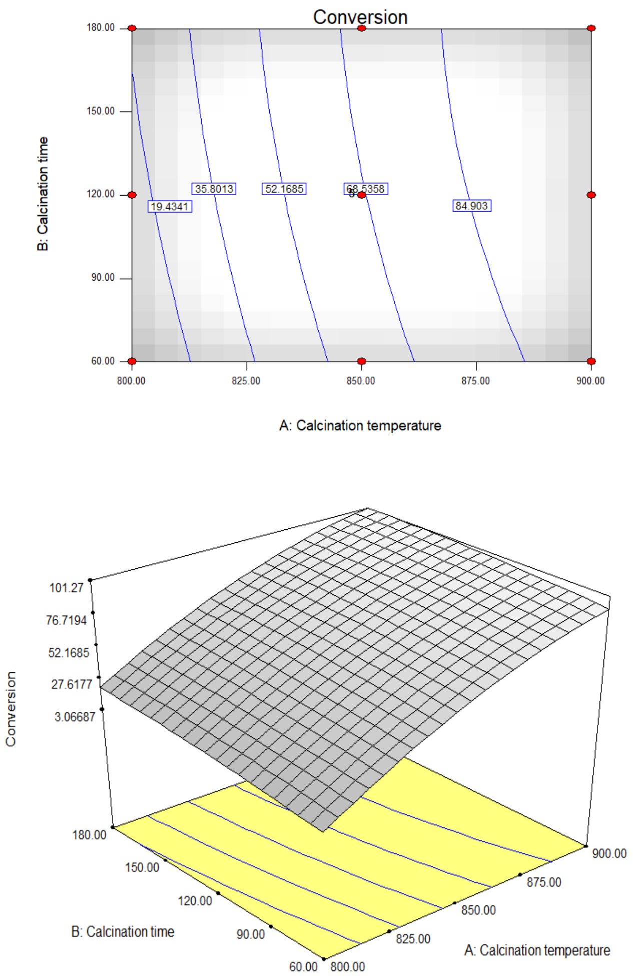

Figure 4 – Response surface plot (Contour and 3 D surface) showing the effect of different factors (X_1: Calcination temperature, X_2: calcination time) for SO_3 yield with TG analysis for quadratic model

Similar trends of an increase in the SO_3 yield from TG and XRF analyses were observed as the calcination temperature was increased at constant times of 60, 120 and 180 minutes illustrated in Figures 5–6 respectively. A significant increase in the SO_3 yield via TG and XRF analyses was experienced as both factors were gradually increased. Similarly, an increase in the SO_3 conversion was experienced as the calcination time was gradually increased from 60 to 180 min at constant calcination temperature of 800, 850 and 900 °C.

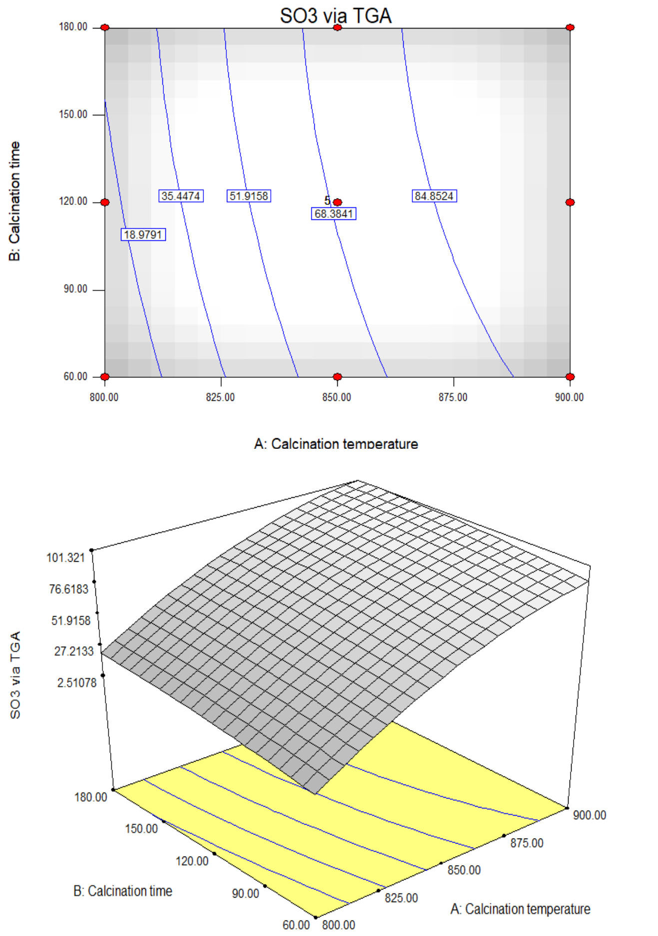

Figure 5 – Response surface plot (Contour and 3 D surface) showing the effect of different factors (X_1: Calcination temperature, X_2: calcination time) for SO_3 conversion for quadratic model

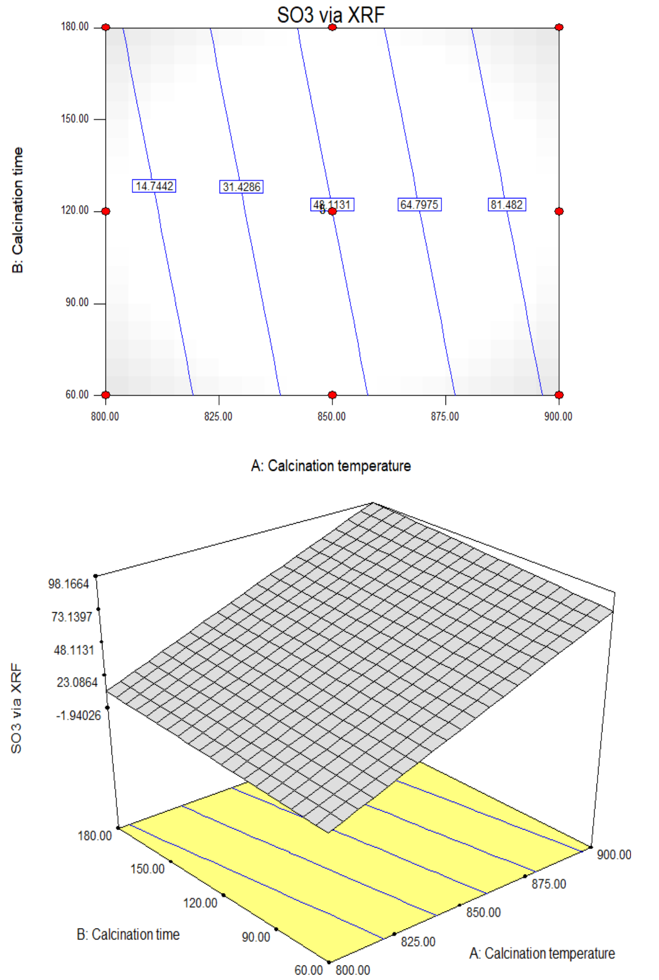

Figure 6 – Response surface plot (Contour and 3D surface) showing the effect of different factors (X_1: Calcination temperature, X_2: calcination time) for SO_3 yield with XRF for quadratic model

Figures 8 and 9 illustrate the effect of calcination time on the SO_3 yield via TG and XRF analysis at various constant calcination temperature. From the predictive model for the determination of the SO_3 via TG analysis, it could be observed that the SO_3 yield increased as the calcination time progressed from 60-180 minutes while the calcination temperature was held constant at 800, 825, 850, 875 and 900 °C respectively. The SO_3 yield via TG analysis increased from 24.32–43.54 %, 49.93–65.67 % as the calcination time progressed from 60–180 minutes at constant calcination temperature of 850 and 900 °C respectively. This increase in SO_3 yield could be attributed to the increase in the duration of calcination stemming from the increase in kinetic energy gained by the molecules to overcome the activation energy resulting in increased SO_3 yield.

Similar trend of an increase in the SO_3 yield via XRF analysis as the calcination time progressed at constant calcination temperature of 800, 825, 850, 875 and 900 °C respectively. The SO_3 yields via XRF analysis were found to be higher compared to those obtained from TG analysis. The values of SO_3 yield via XRF were also significantly close to SO_3 conversion values at various calcination temperatures and time compared to those of SO_3 yield via TG analysis. This could be attributed to the accuracy of the analyses of the SO_3 yield. The increase in yield of SO_3 from the decomposition of alum derived from kaolin clay could be attributed to the increase in amount of kinetic energy required to propagated the decomposition reaction as the temperature was increased or the calcination time progressed [29].

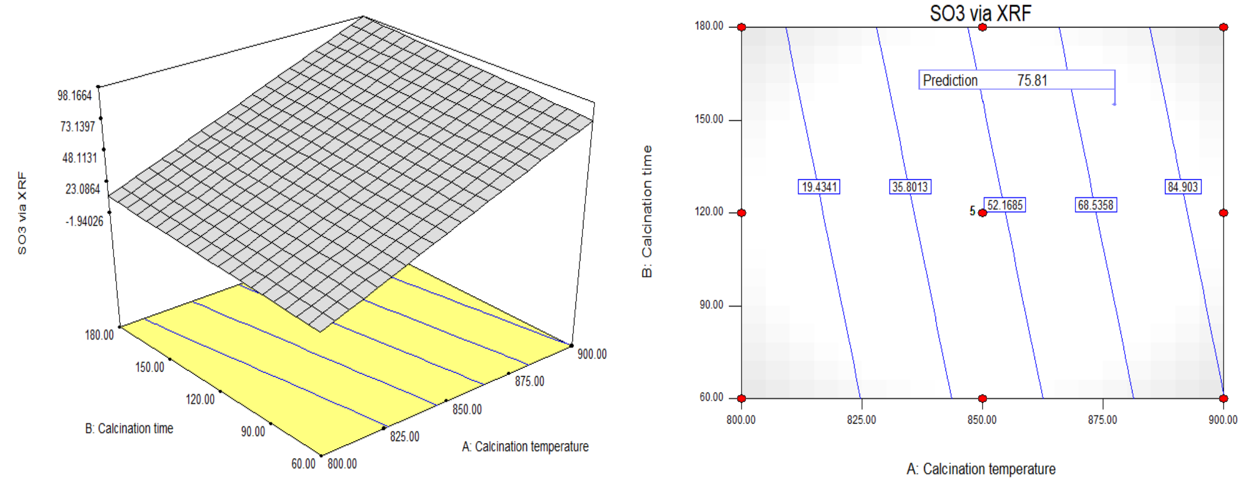

Figure 7 – Response surface plot (3D surface and Contour) indicating the optimal conditions (X_1: Calcination temperature, X_2: calcination time) for SO_3 conversion

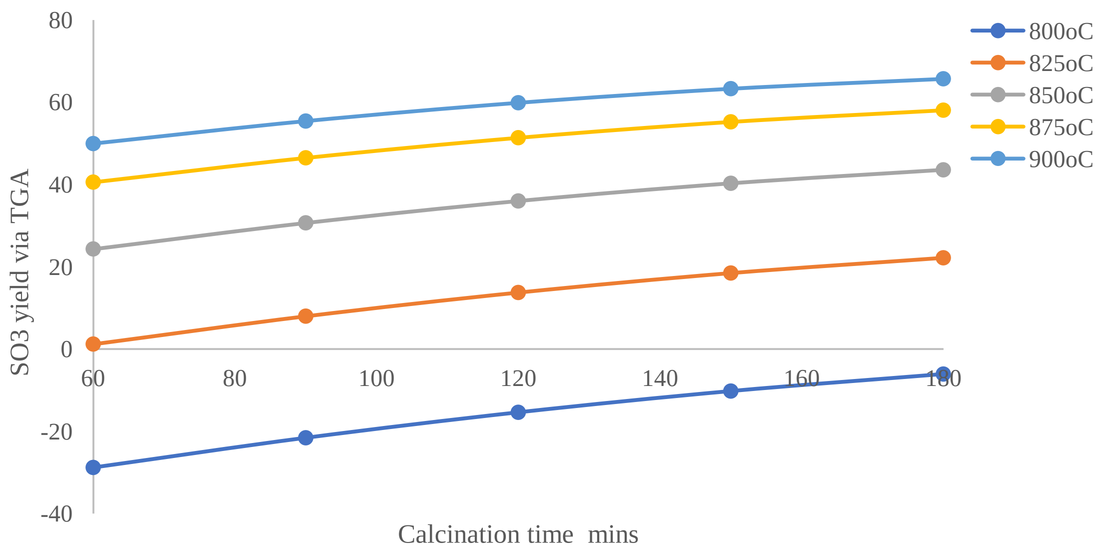

Figure 8 – Effect of calcination time on the SO_3 yield via TG analysis at various calcination temperatures

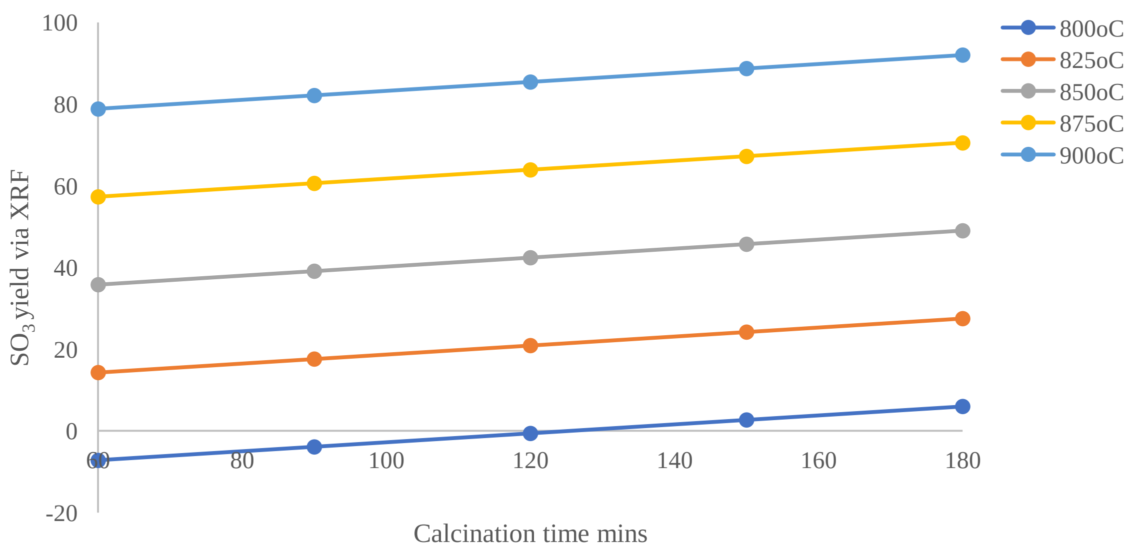

Figure 9 – Effect of calcination time on the SO_3 yield via XRF at various calcination temperatures

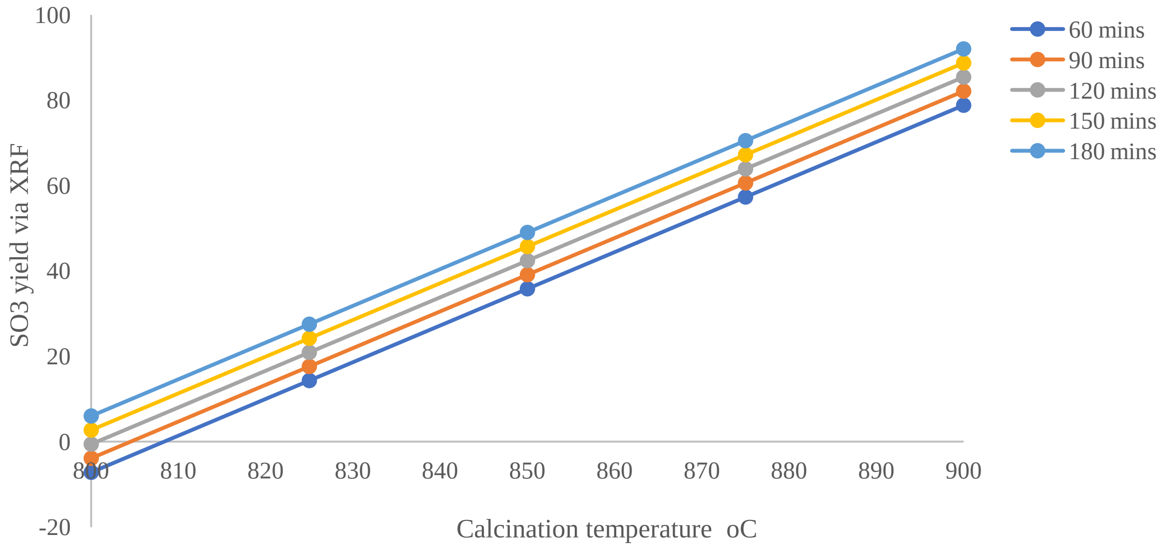

Figure 10 – Effect of calcination temperature on the SO_3 yield via XRF at various calcination times

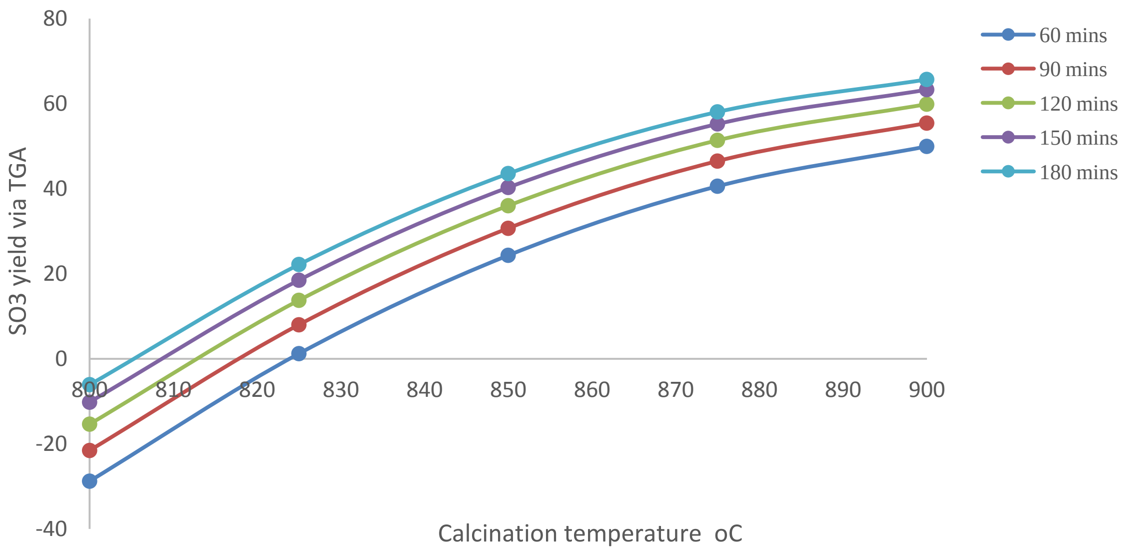

Figure 11 – Effect of calcination temperature on the SO_3 yield via TG analysis at various calcination times

It could be observed in Figure 10 and 11, that as the calcination temperature was gradually increased from 800–900 °C, there was a steady increase in the SO_3 yield for both XRF and TG analyses respectively. On the other hand, the predictive model for the determination of the SO_3 yield via XRF analysis, it could be seen that as the calcination time was held constant at 180 minutes and the calcination temperature was increased from 800–900 °C, the SO_3 yield via XRF increased from 6.01–92.01 %. Similar trend of an increase in the SO_3 yield via XRF was observed for other calcination time at 60, 90, 120 and 150 minutes respectively.

Optimization. Optimization of the production of SO_3 was conducted and the optimal conditions for optimal SO_3 conversion of 90.11 %, SO_3 yield via TG analysis of 91.67 % and SO_3 yield via XRF of 75.81 % at an optimal calcination temperature of 877.43 °C and time of 155.04 minutes. Figures 12–13 indicated similar trend of an increase in the SO_3 conversion and SO_3 yield obtained via TG and XRF analyses as the calcination temperature and time of the aluminum sulfate was simultaneously increased as illustrated by the response surface plots.

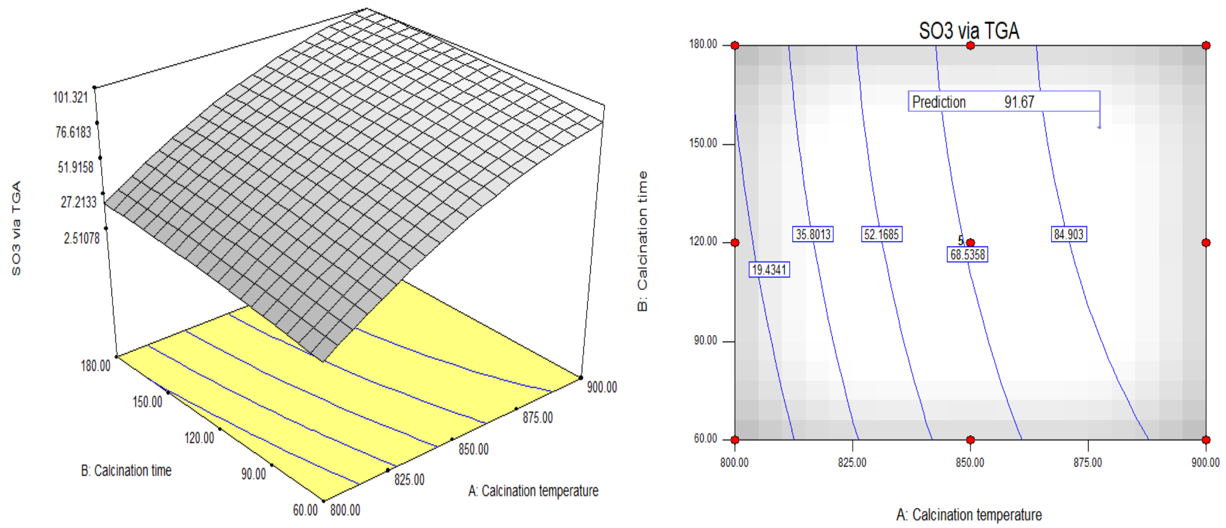

Figure 12 – Response surface plot (3D surface and Contour) indicating the optimal conditions (X_1: Calcination temperature, X_2: calcination time) for SO_3 yield via TG analysis respectively

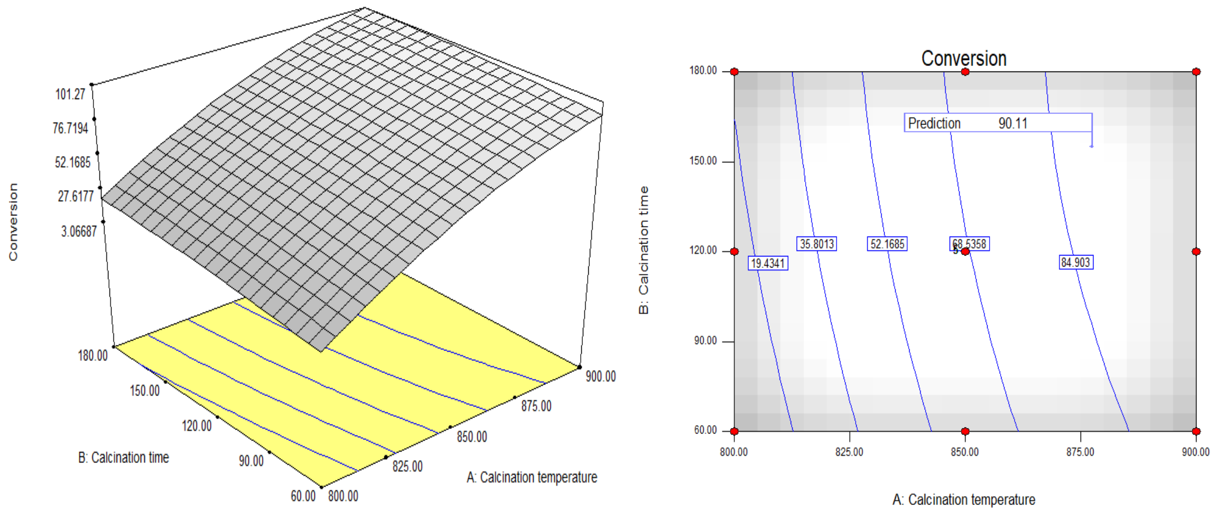

Figure 13 –Response surface plot (3D surface and Contour) indicating the optimal conditions (X_1: Calcination temperature, X_2: calcination time) for SO_3 yield via XRF

CONCLUSION

An increase in the calcination temperature and time between 800–900 °C and 60–180 minutes led to an increase in the SO_3 conversion, SO_3 yield via XRF and TG analyses respectively. Based on experimental results, an empirical relationship between the response and factors was obtained and found SO_3 conversion and SO_3 yield via TG analysis best suited with quadratic models whereas SO_3 yield via XRF satisfied a linear model. The SO_3 yields and conversion were established by the response surface and contour plots of the model-predicted responses. The SO_3 conversion and SO_3 yields via TG and XRF analyses of 90.11 %, 91.67% and 75.81 % were obtained under optimal value of process parameters for calcination temperature of 877.43 °C and time of 155.04 minutes respectively. Analysis of variance for SO_3 conversion and SO_3 yields via TG and XRF analyses indicated a high coefficient of determination value for SO_3 conversion and yields (R^2 =97.8%, R^2_{adj} = 97.06%) (97.77%, R^2_{adj}=97.03) and (R^2 =97.67 R^2_{adj}=97.06) respectively. Thus, a satisfactory agreement of the second-order regression and first order model with the experimental data for TG and XRF analyses respectively. The calcination temperature provided the most significant effect on the SO_3 yields and conversion compared with calcination time. It was also observed from the ANOVA that SO_3 yield via XRF gave the best model with (R^2_{pred} = 91.98%) compared to SO_3 yield via TG analysis (R^2_{pred}=79.99 %) and SO_3 conversion (R^2_{pred}=78.01 %) respectively.

ACKNOWLEDGEMENTS

The authors wish to thank National Metallurgical Development Centre, Jos and the Department of Chemical Engineering of Ahmadu Bello University Zaria for providing infrastructure, facilities and their support to this research work.

CONFLICT OF INTEREST

The authors declared that they have no conflict of interest.

REFERENCES

1. Lerner, L. (2011). *Small-Scale Synthesis of Laboratory Reagents with Reaction Modeling*. New York: CRC Press.
2. Loerting, T., & Liedl, K. R. (2000). Toward elimination of discrepancies between theory and experiment: The rate constant of the atmospheric conversion of SO3 to H2SO4. *Proceedings of the National Academy of Sciences, 97*(16), 8874–8878. doi: 10.1073/pnas.97.16.8874
3. Jadhav, Y., Deshpande, S., & Sindhikar, A. (2018). Manufacturing of Sulphate castor oil (Turkey red oil) by the Sulphonation process. *International Journal of Advanced Research in Science Engineering and Technology, 5*(7), 6384–6389.
4. Dunn, J. P., Koppula, P. R., G. Stenger, H., & Wachs, I. E. (1998). Oxidation of sulfur dioxide to sulfur trioxide over supported vanadia catalysts. *Applied Catalysis B: Environmental, 19*(2), 103–117. doi: 10.1016/s0926-3373(98)00060-5
5. Olubajo, O., Waziri, S., Aderemi, B. (2014). Kinetic of the decomposition of alum sourced from Kankara Kaolin. *International Journal of Engineering Research and Technology, 3*(2), 1629–1635.
6. Azami, M., Bahram, M., Nouri, S., & Naseri, A. (2012). Central composite design for the optimization of removal of the azo dye, methyl orange, from waste water using fenton reaction. *Journal of the Serbian Chemical Society, 77*(2), 235–246. doi: 10.2298/jsc110315165a
7. Khuri, A., & Mukhopadhyay, S. (2010). Response surface methodology. In E. J. Wegman, Y. H. Said, & D. W. Scott (Eds.), *Computational Statistics* (pp. 128–149). Hoboken: John Wiley and Sons.
8. Said, Kh., & Amin, M. (2015). Overview on the Response Surface Methodology (RSM) in Extraction Processes. *Journal of Applied Science & Process Engineering, 2*(1), 8–17.
9. Hamzaoui, A. H., Jamoussi, B., & M'nif, A. (2008). Lithium recovery from highly concentrated solutions: Response surface methodology (RSM) process parameters optimization. *Hydrometallurgy, 90*(1), 1–7. doi: 10.1016/j.hydromet.2007.09.005
10. Giménez, M., Blanes, P., Hunzicker, G., & Garro, O. (2009). Application of a central composite design to the determination of inorganic and organic arsenic species in water by liquid chromatography–hydride generation– atomic absorption spectrometry. *AFINIDAD, LXVI*(540), 126–133.
11. Aybastıer, Ö., Şahin, S., Işık, E., & Demir, C. (2011). Determination of total phenolic content in Prunella L. by horseradish peroxidase immobilized onto chitosan beads. *Analytical Methods, 3*(10), 2289. doi: 10.1039/c1ay05218g
12. Adeleke, O. A., Latiff, A. A. A., Saphira, M. R., Daud, Z., Ismail, N., Ahsan, A., … Hijab, M. (2019). Locally Derived Activated Carbon From Domestic, Agricultural and Industrial Wastes for the Treatment of Palm Oil Mill Effluent. *Nanotechnology in Water and Wastewater Treatment*, 35–62. doi: 10.1016/b978-0-12-813902-8.00002-2
13. Olubajo, O. O., Makarfi, I. Y., & Odey, O. A. (2019). Prediction of Loss on Ignition of Ternary Cement Containing Coal Bottom Ash and Limestone Using Central Composite Design. *Path of Science, 5*(8), 2010–2019. doi: 10.22178/pos.49-3
14. Elksibi, I., Haddar, W., Ben Ticha, M., gharbi, R., & Mhenni, M. F. (2014). Development and optimisation of a non conventional extraction process of natural dye from olive solid waste using

response surface methodology (RSM). *Food Chemistry, 161*, 345–352. doi: 10.1016/j.foodchem.2014.03.108

15. Ravikumar, K., Ramalingam, S., Krishnan, R., & Balu, B. (2006). Application of response surface methodology to optimize the process variables for Reactive Red and Acid Brown dye removal using a novel adsorbent. *Dyes and Pigments, 70*(1), 18–26. doi: 10.1016/j.dyepig.2005.02.004
16. Wong, Y. C., Tan, Y. P., Taufiq-Yap, Y. H., & Ramli, I. (2015). An Optimization Study for Transesterification of Palm Oil using Response Surface Methodology (RSM). *Sains Malaysiana, 44*(2), 281–290. doi: 10.17576/jsm-2015-4402-17
17. Chaudhary, G., Kumar, M., Verma, S., & Srivastav, A. (2014). Optimization of Drilling Parameters of Hybrid Metal Matrix Composites Using Response Surface Methodology. *Procedia Materials Science, 6*, 229–237. doi: 10.1016/j.mspro.2014.07.028
18. Silva, G. F., Camargo, F. L., & Ferreira, A. L. O. (2011). Application of response surface methodology for optimization of biodiesel production by transesterification of soybean oil with ethanol. *Fuel Processing Technology, 92*(3), 407–413. doi: 10.1016/j.fuproc.2010.10.002
19. Olubajo, O., Osha, O., Elnatafy, U., & Adamu, H. (2017). *A study on the physico-mechanical properties and the hydration of ordinary cement blended with limestone and coal bottom ash* (Doctoral thesis); Abubakar Tafawa Balewa University Bauchi.
20. De Weerdt, K., Kjellsen, K. O., Sellevold, E., & Justnes, H. (2011). Synergy between fly ash and limestone powder in ternary cements. *Cement and Concrete Composites, 33*(1), 30–38. doi: 10.1016/j.cemconcomp.2010.09.006
21. Myers, R., Montegomery, D., & Anderson, C. (2009). *Response Surface Methodology: Process and Product Optimization using Designed Experiment* (3rd ed.). Hoboken: Wiley & Sons Inc.
22. Koocheki, A., Taherian, A., Razavi, S., & Bostan, A. (2009). Response surface methodology for optimization of extraction yield, viscosity, and hue and emulsion stability of mucilage extracted from Lepidium perfoliatum Seeds. *Food Hydrocolloids, 23*, 2369–2379.
23. Chauhan, B., & Gupta, R. (2004). Application of statistical experimental design for optimization of alkaline protease production from Bacillus sp. RGR-14. *Process Biochemistry, 39*(12), 2115–2122. doi: 10.1016/j.procbio.2003.11.002
24. Abdulkarim Ikara, I. (2019). Predicting CBR Values of Black Cotton Soil Stabilized with Cement and Waste Glass Admixture Using Regression Model. *American Journal of Traffic and Transportation Engineering, 4*(1), 31. doi: 10.11648/j.ajtte.20190401.15
25. Zaibunnisa, A. H., Norashikin, S., Mamot, S., & Osman, H. (2009). An experimental design approach for the extraction of volatile compounds from turmeric leaves (Curcuma domestica) using pressurised liquid extraction (PLE). *LWT - Food Science and Technology, 42*(1), 233–238. doi: 10.1016/j.lwt.2008.03.015
26. Arsenovic, M., Pezo, L., & Radojevic, Z. (2012). Response surface method as a tool for heavy clay firing process optimization: Roofing tiles. *Processing and Application of Ceramics, 6*(4), 209–214. doi: 10.2298/pac1204209a
27. Dutta, S., Ghosh, A., Moi, S. C., … Saha, R. (2015). Application of Response Surface Methodology for Optimization of Reactive Azo Dye Degradation Process by Fenton's Oxidation. *International Journal of Environmental Science and Development, 6*(11), 818–823. doi: 10.7763/ijesd.2015.v6.705
28. Ramamoorthi, M., Rengasamy, M. (2015). Performance analysis of Mustard and Pongamia Methyl Ester Blends with diesel in CI engine. *Journal of Chemical and Pharmaceutical Science, 4*(4), 257–259.
29. Dockery, G. (2017, April 24). *The effect of temperature on activation energy*. Retrieved from https://sciencing.com/effect-temperature-activation-energy-5041227.html